

REACTIVE OXYGEN SPECIES AND P38 MAPK ACTIVATE BAX TO INDUCE MITOCHONDRIAL CYTOCHROME C RELEASE AND APOPTOSIS IN RESPONSE TO MALONATE

Gomez-Lazaro M., Galindo MF., Melero-Fernandez de Mera RM, Fernandez-Gómez FJ., Concannon CG., Segura MF, Comella JX, Prehn JHM. and Jordan J.

Grupo de Neurofarmacología. Departamento de Ciencias Médicas. Facultad de Medicina. Universidad Castilla-La Mancha. M. G-L, M.F G, R.M. M-FM; F.J. F-G., J.J.

Department of Physiology and RCSI Neuroscience Research Centre, Royal College of Surgeons in Ireland, 123 St Stephen's Green, Dublin 2, Ireland. CGC, JHMJ

Cell Signaling and Apoptosis group. Departament de Ciències Mèdiques Bàsiques. Univeristy of Lleida and Hospital Arnau de Vilanova. Lleida (Spain). MF S, JXC.

Centro Regional de Investigaciones Biomedicas. Albacete. Spain M. G-L, M.F G, R.M. M-FM; F.J. F-G., J.J.

Running title: Pathways involved in malonate-induced Bax translocation.

To whom all correspondence should be sent at the following address:

Joaquin Jordán, Grupo de Neurofarmacología. Departamento de Ciencias Médicas.
Facultad de Medicina. Universidad Castilla-La Mancha. 02006-Albacete. Spain. Tel
34-967599200. Fax 34-967599327. E-Mail joaquin.jordan@uclm.es

Number of text pages: 21

Number of tables: 0

Number of figures: 7

Number of references: 40

Number of words in the Abstract: 155

Number of words in the Introduction: 470

Number of words in the Discussion: 553

Abbreviations:

$\Delta\Psi_m$, mitochondrial transmembrane potential; CM-H₂DCFDA, 2',7'-

dichlorodihydrofluorescein diacetate; DIV, days *in vitro*; GFP, Green fluorescent

protein; MDA, Malondialdehyde; MEF, mouse embryonic fibroblasts; ROS, reactive

oxygen species; TMRE, tetramethylrhodamine ethyl ester.

ABSTRACT

Malonate, an inhibitor of mitochondrial complex II, is a widely used toxin to study neurodegeneration in Huntington's disease and ischemic stroke. We have previously shown that malonate increased reactive oxygen species (ROS) production in human SH-SY5Y neuroblastoma cells, leading to oxidative stress, cytochrome-c release, and apoptotic cell death. Expression of a Green Fluorescent Protein-Bax fusion protein in SH-SY5Y neuroblastoma cells demonstrated a Bax redistribution from the cytosol to mitochondria after 12 – 24 h of malonate treatment that coincided with mitochondrial potential collapse and chromatin condensation. Inhibition of Bax translocation using furosemide, as well as Bax gene deletion afforded significant protection against malonate-induced apoptosis. Further experiments revealed that malonate induced a prominent increase in the level of activated p38 MAP kinase, and that treatment with the p38 MAP kinase inhibitor SKF86002 potently blocked malonate-induced Bax translocation and apoptosis. Treatment with vitamin E diminished ROS production, reduced the activation status of p38 MAP kinase, inhibited Bax translocation and protected against malonate-induced apoptosis. Our data suggest that malonate-induced ROS production and subsequent p38 MAP kinase activation mediates the activation of the pro-apoptotic Bax protein to induce mitochondrial membrane permeabilisation and neuronal apoptosis.

Compromised mitochondrial function has been observed in several neurodegenerative disorders, and inhibitors of mitochondrial respiration are frequently used to mimic neurodegenerative disorders (Browne and Beal, 2002). Intrastratial injection of the mitochondrial complex II inhibitor malonate induces striatal lesions similar to those described in cerebral ischemia and Huntington's disease (Brouillet et al. 1995). The mechanisms that account for these neurotoxic effects remain to be fully elucidated (Ferber et al., 1999). It has been proposed that malonate toxicity involves depletion of striatal ATP (Beal et al., 1993), resulting in neuronal depolarization and a secondary excitotoxic neuron loss (Beal et al 1994). It has also been reported that malonate is capable of inducing a caspase-dependent apoptotic cell death (Schulz et al., 1998).

Mitochondria are being considered a main link between cellular stress signals activated during acute and chronic nerve cell injury and the execution of apoptotic and necrotic cell death (Jordan et al. 2004; Mattson and Kroemer, 2003). ATP depletion, pathophysiological increases in intracellular calcium (Ca^{2+}) and enhanced reactive oxygen species (ROS) production frequently occur during necrotic cell death and can trigger an increase in the permeability of the inner mitochondrial membrane. This process is believed to involve the formation of a multiprotein channel referred to as mitochondrial permeability transitory pore (MPTP) (Bernardi, 1999) which triggers the release of solutes up to 1500 Da from the mitochondrial matrix into the cytoplasm. Apoptotic events in contrast can cause an increase in the permeability of the outer mitochondrial membrane (Green, 2006). This process triggers the release of intermembrane space proteins into the cytoplasm, including cytochrome c, Smac/DIABLO, and apoptosis-inducing factor. Cytochrome-C and Smac/DIABLO are capable of activating a family of cytosolic cysteine proteases, the caspases, while

AIF has been implicated in caspase-independent forms of apoptosis (Martinou et al., 2002; Goldstein et al., 2002).

The Bax protein has been identified as a key pro-apoptotic Bcl-2 family protein during neuronal apoptosis. Bax normally resides in the cytosol and translocates to mitochondria in response to a variety of apoptotic stimuli, including cerebral ischemia (Cao et al., 2001; Putcha et al., 1999; Wolter et al., 1997). The pro-apoptotic action of Bax is believed to be mediated by its insertion into the outer mitochondrial membrane where it might directly form channels or regulate the activity of pre-existing channels (Goping et al., 1998; Sharpe et al., 2004). This step requires a conformational change in the Bax protein. The upstream events that induce this conformational change are still largely unknown. Previously, we have demonstrated that malonate causes apoptosis of human SH-SY5Y neuroblastoma cells, involving increased reactive oxygen species production, oxidative stress and mitochondrial cytochrome C release (Fernandez-Gomez et al., 2005). In the present study we were interested in studying the requirement of Bax for malonate-induced apoptosis and in elucidating the signalling pathways involved in malonate-induced Bax activation.

MATERIALS AND METHODS

Cell culture and drug treatment procedures- SH-SY5Y cultures were grown as previously described (Jordan et al., 2004) (in Dulbecco's modified Eagle's medium (DMEM) supplemented with 2 mM L-glutamine, penicillin (20 units/mL), streptomycin (5 µg/mL), and 15% (v/v) fetal bovine serum (Gibco, Gaithersburg, MD, USA). Cells were grown in a humidified cell incubator at 37°C under a 5% CO₂ atmosphere. For GFP-Bax translocation and viability experiments, cells were plated on glass coverslip at 2.9×10^5 cells/cm² and allowed to attach overnight. Immediately before malonate

addition, dilutions of malonate were made in phosphate-buffered saline (PBS) and added to fresh cell culture medium to achieve the required concentration.

Primary cultures of cerebellar granule neurons were obtained from dissociated cerebella of 7-8-day-old rats (Fernandez-Gomez et al., 2006). Dissection and dissociation were carried out in Basal Medium Eagle (BME; Life Technology). Tissues were incubated with trypsin for 20 min at 37°C and dissociated by trituration in a medium containing DNase and trypsin. Cells were plated on 60-mm plastic Petri dishes pre-coated with poly-L-lysine (10 µg/ml) at a concentration of 8×10^6 cells/ml in BME containing 25 mM KCl, 10% de-complemented fetal calf serum (FCS; Life Technology), glutamine, and antibiotics. Cytosine-β-D-arabino-furanoside (Ara-C) (10 µM) was added at 3 days *in vitro* (DIV) to prevent the growth of non-neuronal cells. All experiments were carried out after 7 days in culture.

Transfection- Cells were plated 24h before transfection at a density of 5.3×10^4 cells/cm², on poly D-lysine-coated glass slides. Transfection was achieved using LipofectamineTM reagent (Invitrogen, Carlsbad, CA) according to the manufacturer's protocol. Cells were transfected with the following plasmids encoding caspase-9 dominant-negative mutant caspase-9 (C287A; casp 9DN, a gift from Ding HF, Medical College of Ohio, Toledo, Ohio), Bcl-2, Bcl-xL and p35 (Dr J Merino Universidad de Santander), GFP (pGFP-C1; CLONTECH Laboratories, Inc.), GFP-Bax (Poppe et al., 2002). After 4h incubation the transfection mixture was removed and replaced with fresh complete medium.

Confocal microscopy- For time-lapse analysis, cells were grown in 24mm poly D-lysine-coated glass slides and mounted in a chamber for confocal microscopy with Krebs HEPES buffer with the following ionic composition (in mM): NaCl 140, KCl 5.9, MgCl₂ 1.2, HEPES 15, glucose 10, CaCl₂ 2.5, pH 7.4. Images were captured with a

Leica microscope using a 63X 1.4 NA objective. The excitation wavelengths for GFP and TMRE were 488 and 543nm respectively. Images were taken for an hour every 5 minutes for control cells, and treated cells were injured with malonate after the first photograph.

Mitochondrial potential - The cationic, lipophilic dye tetramethylrhodamine ethyl ester (TMRE; Molecular Probes) enters cell in a form of an ester which is subsequently hydrolysed and the product, tetramethylrhodamine, is accumulated in mitochondria due to a high membrane potential. Cell cultures were washed in K-H, and incubated at 37°C for 30 minutes in with TMRE (0.1 μ M). Cells were then washed with K-H and resuspended in K-H. Cell fluorescence was analyzed by confocal microscopy as it has been described above.

Detection of peroxides / reactive oxygen species – We used the oxidation-sensitive fluorescent dye 2',7'-dichlorodihydrofluorescein diacetate (CM-H₂DCFDA) to measure the production of ROS, mainly hydrogen peroxide and hydroxyl radicals. DCFH-DA is deacetylated by esterases to dichlorofluorescein (DCFH). This nonfluorescent product is then converted by reactive species into DCF, which can easily be visualized by fluorescence at 530 nm when excited at 485 nm. SH-SY5Y cells seeded in 96-well culture plates were incubated with DCFH-DA (10 μ g/ml) for 5 min, and fluorescence intensity was measured in a Spectra Max Gemini XS (Molecular Devices). Average ROS production (relative to level of vehicle-treated controls) was calculated from four individual wells in at least three independent platings.

Assessment of apoptotic cell death - SH-SY5Y cells or cerebellar granule cells were plated on poly D-lysine-coated glass slides. For cell death assay, nuclei were

stained with 0.5 µg/ml of Hoechst 33258. Uniformly stained nuclei were scored as healthy, viable neurons. Condensed or fragmented nuclei were scored as apoptotic.

Western blot - SH-SY5Y cell cultures were washed with cold PBS twice and then collected by mechanical scraping with 1 ml of PBS per tissue culture dish. The suspension was centrifuged at 12,000 –14,000 rpm for 5 min. The supernatant was discarded, and the pellet was brought up in 150 µl of sample buffer. The protein from each condition was quantified spectrophotometrically (Micro BCA Protein Reagent Kit, Pierce, Rockford, IL), and an equal amount of protein (30 µg) was loaded onto 10 % SDS-PAGE gels. After electrophoresis, proteins were transferred to Immobilon PVDF membranes. Non-specific protein binding was blocked with Blotto [4% w/v non-fat dried milk, 4% bovine serum albumin (Sigma) and 0.1% Tween 20 Sigma]] in PBS for 1 h. The membranes were incubated with anti-p53 [1:1000 dilution of anti-mouse monoclonal (Pab240) sc-99 Santa Cruz], anti-pan p38 and anti-phospho-p38 (1:1000 dilution of polyclonal) overnight at 4 °C. After washing with Blotto, the membranes were incubated with a secondary antibody (1:5000 dilution of peroxidase-labeled anti-mouse, Promega, Madison, WI) in Blotto. The signal was detected using an enhanced chemiluminescence detection kit (Amersham ECL RPN 2106 Kit). Immunoblots were developed by exposure to x-ray film (Eastman-Kodak, Rochester, NY).

Lipid peroxidation - Lipid peroxidation was measured by determining malondialdehyde (MDA) levels. Each sample (8×10^6 cells) was collected in 100µL of ice-cold 20 mM BTris–HCl buffer, pH 7.4, and sonicated. Amounts of MDA were determined in the cellular extracts using a Lipid Peroxidation Assay Kit from

Calbiochem (No. 437634) based on the condensation reaction of the chromogene 1-methyl-2-phenylindole with either MDA. The stable chromophores were determined at 586 nm. Results are expressed as percent of ng MDA per mg protein found in untreated cell cultures.

Statistics - The results were expressed at the mean +/- SD of at least three independent experiments. Student's two-tailed, unpaired t test was used, and values of $P < 0.05$ were considered to be significant. When comparing more than two conditions statistically significant differences between groups were determined by ANOVA followed by a Newman-Keuls post hoc analysis. The level of statistical significance was set at $P < 0.05$.

RESULTS

Malonate induces cell death through the mitochondrial apoptosis pathway - In the mitochondrial apoptosis pathway, the release of cytochrome-C triggers the formation of a caspase-3 activating complex, the apoptosome. Caspase-3 was activated in SH-SY5Y neuroblastoma cells challenged with malonate as evidenced by Western blot analysis. As shown in Figure 1A, the addition of 50 mM malonate to SH-SY5Y cell cultures resulted in the activation of caspase-3 after 12 – 24 h of treatment. To analyse whether the mitochondrial pathway participated in malonate-induced cell death we co-transfected SH-SY5Y cells with a GFP expression vector and Bcl-2 or Bcl-xL expression vectors. Bcl-2 and Bcl-xL are known to inhibit mitochondrial cytochrome-C release by neutralizing the pro-apoptotic activity of Bax and Bak. 24 h after transfection, cell cultures were treated with malonate (50 mM, 12

h) and the effect of malonate on the viability of the GFP-positive SH-SY5Y cells was determined. As shown in figure 1B, the overexpression of Bcl-2 or Bcl-xL potently abrogated the cytotoxic effect of malonate in the SH-SY5Y cells. Similar results were found in cell cultures transfected with the baculoviral broad spectrum caspase inhibitor p35. The apoptosome is comprised of APAF-1, cytochrome-C and caspase-9. Potent inhibition of malonate-induced apoptosis was also observed when we inhibited the function of endogenous caspase-9 by overexpression of a dominant-negative mutant form (Caspase-9 DN) (Figure 1B). Together, these results indicate that malonate activates the mitochondrial apoptosis pathway in human SH-SY5Y neuroblastoma cells.

Malonate induces Bax translocation to mitochondria- By using a Green fluorescent protein (GFP)-Bax fusion protein, we addressed the question whether Bax translocation was involved in malonate-induced apoptosis. As shown in Figure 2, confocal imaging studies revealed that in untreated SH-SY5Y cells, GFP-Bax was distributed evenly in the cytosolic compartment. After 12 h of malonate treatment, we observed a marked change in GFP-Bax fluorescence from a diffuse, cytosolic to a clustered, mitochondrial pattern. Approximately 35 % of the malonate-challenged cells displayed a GFP-Bax translocation after 12 h. Use of the mitochondrion-selective dye Mito-Tracker Red (Figure 2 A-C) demonstrated that the clustered, punctuate GFP-Bax distribution colocalized with mitochondria. Disruption of mitochondrial transmembrane potential ($\Delta\Psi_m$) has been demonstrated to occur downstream of mitochondrial cytochrome-C release (Waterhouse et al., 2001). By analyzing tetramethylrhodamine ethyl ester fluorescence intensities we studied $\Delta\Psi_m$ changes in cells exhibiting either a clustered or diffuse GFP-Bax distribution. By 12 h

after malonate treatment, we found that clustered punctuated GFP-Bax cells showed an approximately 75 % decrease in TMRE fluorescence compared to those cells with cytoplasmic diffuse GFP-Bax distribution (n = 114 cells). In malonate-treated cells where Bax translocation had not yet occurred, mitochondrial potential remained at the level observed in untreated cells (Figure 2D). Epifluorescence observation suggested that cells with a clustered GFP-Bax fluorescence also exhibited a nuclear apoptotic morphology, and analyzed by chromatin using Hoechst 33342 (Figure 2 E).

Bax is required for malonate-induced apoptosis- To determine the Bax involvement in malonate-induced apoptosis, we blocked Bax translocation using the chloride channel inhibitor furosemide (Karpnich et al., 2002). As shown in Figure 3A, a three h pre-treatment with 10 μ M furosemide significantly reduced Bax translocation and afforded significant protection to the SH-SY5Y cells treated for 12 h with 50 mM malonate.

In the next set of experiments, we addressed the question whether Bax was required for malonate-induced apoptosis. Western blotting analysis of lysates prepared from mouse embryonic fibroblasts (MEF) cultures revealed that malonate failed to activate caspase-3 in cells derived from Bax-deficient mice (Figure 3B). Indeed, the lack of Bax protein conferred resistance against malonate toxicity, as Bax^{-/-} MEFs were protected against malonate-induced apoptosis (Figure 3C).

Inhibition of ROS production inhibits malonate-induced Bax translocation and apoptosis - We have previously showed that ROS production is increased in SH-SY5Y cells cultures challenged with malonate (Fernandez-Gomez et al., 2005). To investigate whether this increased ROS production is functionally linked to malonate-

induced Bax translocation, we treated SH-SY5Y neuroblastoma cells with the ROS scavenger vitamin E. A one-h pre-treatment with 50 μ M vitamin E significantly inhibited the formation of peroxides detected with the fluorescent indicator CM-H₂DCFDA (Fig 4A). Pre-treatment with vitamin E also reduced malonate-induced GFP-Bax translocation compared to vehicle-treated controls (Figure 4B). We next tested whether vitamin E treatment also conferred protection against malonate-induced apoptosis. Consistent with the effect on Bax-translocation, a pre-treatment for 1 h with 50 μ M vitamin E afforded significant protection against malonate-induced apoptosis (Figure 4C). A similar protection was observed in vitamin E-pre-treated cultured cerebellar granule neurons exposed to malonate (Fig. 4D).

ROS are an important source of toxin-, ischemia-, and age-related DNA damage (Lombard et al., 2005). Indeed, there is growing evidence for a pivotal function of p53 in neuronal death (Gomez-Lazaro et al., 2004). To elucidate the participation of p53 in malonate-induced cell death, we tested whether malonate induced an increase in the total p53 protein levels in SH-SY5Y cell cultures. Western blotting analysis revealed that malonate did not increase p53 protein levels at any time point investigated (Figure 5A). We found that SH-SY5Y neuroblastoma cells treated with 6-hydroxydopamine on the contrary showed a significant increase in the cellular p53 levels (Biswas et al., 2005). To confirm a lack of p53 in the signaling pathways leading to malonate-induced cell death, we also performed a set of experiments in p53-deficient MEFs (p53 ^{-/-}MEF). The lack of p53 did not afford a significant protection against malonate-induced apoptosis (Figure 5B). These experiments suggested that the effects of ROS on Bax activation and cell death were independent of p53.

p38 MAP kinase triggers Bax translocation and apoptotic cell death in response to malonate - The p38 MAP kinase participates in several apoptosis pathways, mediating Bax activation and translocation (Ghatan et al., 2000). To analyze whether p38 MAPK was activated by malonate, SH-SY5Y cells were challenged with malonate and cytoplasmic extracts were assayed by Western blotting using a phospho-specific antibody recognizing active p38 MAP kinase (Sanchez-Prieto et al., 2002). Protein extracts from SH-SY5Y cells challenged with 50 mM malonate showed a marked increase in the phosphorylation status of p38 MAPK (Figure 6A). Maximal increases in p38 MAPK phosphorylation occurred after 1 h of treatment. Phosphorylation levels slowly declined subsequently, returning to basal levels after 12 h. Next, we employed the p38 MAP kinase inhibitor SKF86002, to study the relevance of p38 MAP kinase activation in malonate-induced Bax translocation. At 10 μ M, SKF86002 has been shown to inhibit all p38 MAPK isoforms, α , β , δ , and γ . SH-SY5Y cell cultures were pre-treated for 12 h with 10 μ M SKF86002. As shown in Figure 6 B-C, SKF86002 potently prevented the appearance of cells showing a clustered GFP-Bax fluorescence. Importantly, SKF86002 pre-treatment also prevented apoptosis of SH-SY5Y cells treated with malonate (Figure 6D). A similar, potent protection was observed in SKF86002 pre-treated cultured cerebellar granule neurons exposed to malonate (Fig. 4D).

Finally, we determined whether ROS participated in the activation of p38 MAP kinase in response to malonate. Interestingly, a pre-treatment with the anti-oxidant vitamin E reduced the early accumulation of active p38 MAP kinase (Fig. 7A) after 0.5 and 3 h of malonate treatment, suggesting that ROS are required for malonate-induced p38 MAP kinase activation.

It has also been reported that a secondary increase in ROS production can occur late during apoptosis and downstream of mitochondrial cytochrome c release (Luetjens et al., 2000; Düßmann et al., 2003). In agreement with these findings, the levels of malondialdehyde (MDA), a marker for oxidative stress (Esterbauer et al., 1991), were reduced at a later stage (12 h after addition of malonate) in MEF cells treated with the p38 kinase inhibitor SKF86002 compared to vehicle-treated controls (Figure 7B). The levels of MDA in MEFs challenged with 50 mM malonate were also significantly reduced in cells derived from Bax-deficient mice (Figure 7B).

Finally, to confirm the existence of a functionally separated primary and secondary increase in ROS production in more detail, we investigated the effects of vitamin E and SKF86002 pre-treatment on ROS production in SH-SY5Y neuroblastoma cells both at 1 h (early increase) and 12 h (late increase). As expected, pre-treatment with the p38 kinase inhibitor significantly reduced the late increase in ROS production, but had no effect on the early increase (Fig. 7C). In contrast, pre-treatment with vitamin E reduced ROS formation at both time points.

DISCUSSION

In this study we provide evidence that malonate-induced apoptosis of SH-SY5Y neuroblastoma cells is mediated via the pro-apoptotic Bcl-2 family protein Bax. We also demonstrate that both ROS and p38 MAP kinase are required to activate Bax and apoptosis in SH-SY5Y cells and primary cerebellar granule neurons in response to malonate, and that this may occur through functionally interacting signalling pathways.

Cytochrome c release during apoptosis results from the permeabilisation of the mitochondrial outer membrane, a process mediated via activation of the pro-apoptotic, multidomain Bcl-2 family members Bax and Bak. In our study, malonate induced apoptosis was highly dependent on the expression of Bax with apoptosis very significantly impaired in Bax deficient cells. Furthermore, overexpression of the Bax antagonists Bcl-2 and Bcl-X_L, as well as a dominant negative caspase-9, was sufficient to suppress malonate induced apoptosis. This requirement for Bax expression is surprising given that Bax and Bak have functionally redundant roles in a variety of cell death models (Kuwana et al., 2005). However, evidence suggests that neurons express a tissue specific truncated isoform of Bak, N-Bak, which may lack the pro-apoptotic function of full length Bax (Uo et al., 2005). Translocation and clustering of Bax at mitochondria was clearly evident following malonate treatment. Indeed, Bax translocation appeared to be a prerequisite step in malonate-induced apoptosis as a pre-treatment of SH-SY5Y cells with furosemide, which has been shown to inhibit Bax translocation (Lin et al., 2005), also reduced the extent of malonate-induced apoptosis. However, it should also be mentioned that furosemide did not result in a complete inhibition of cell death. Indeed, it has previously been suggested that translocation of roughly 20% of the cellular Bax to the mitochondria may be sufficient to induce apoptosis (Annis et al. 2001).

Several mechanisms have been proposed to account for Bax conformational change responsible for its redistribution. Transcriptional or post-translational activation of BH3 only proteins such as Bid, Bim and PUMA can activate Bax directly or indirectly by binding to and neutralizing the function of Bcl-X_L and Bcl-2. Bax activation may be triggered by modifications in intracellular pH (Khaled et al., 1999) or by phosphorylation of critical amino acid residues by JNK and pK38 MAP kinases

(De Chiara et al., 2006). Malonate produced a marked increase in the phosphorylation of p38 MAP kinase in SH-SY5Y cells. Furthermore, use of the p38 MAP kinase inhibitor, SKF86002, potently inhibited Bax translocation and offered significant protection against malonate-induced apoptosis. Indeed, there is a significant body of evidence suggesting that p38 MAPK activation plays an important role during excitotoxic and neurodegenerative processes (Cao et al., 2004). In addition to the p38 MAPK inhibitor, treatment of SH-SY5Y cells with the antioxidant vitamin E also inhibited Bax translocation resulting in decreased levels of apoptosis. Interestingly, the inhibition of ROS levels ameliorated the effect of malonate on p38 MAP kinase phosphorylation, suggesting that malonate activates ROS which subsequently activate p38 kinase (Ghatan et al., 2000; Choi et al., 2004).

In summary we demonstrate that malonate is able to induce mitochondrial cytochrome c releases through the redistribution of Bax, and that this event is mediated by ROS and the p38 MAP kinase pathway. Interfering with signalling pathways activated either by modulating the accumulation of ROS or by pharmacological inhibition of p38 MAP kinase may afford protection against malonate toxicity. These findings may have important therapeutic implications for the treatment of disorders such as HD and ischaemic stroke.

Acknowledgments

We are grateful to Remedios Sanchis for technical assistance.

REFERENCES

Annis MG, Zamzami N, Zhu W, Penn LZ, Kroemer G, Leber B, and Andrews DW (2001) Endoplasmic reticulum localized Bcl-2 prevents apoptosis when redistribution of cytochrome c is a late event. *Oncogene* **20**:1939-1952.

Beal MF, Brouillet E, Jenkins B, Henshaw R, Rosen B, and Hyman BT (1993) Age-dependent striatal excitotoxic lesions produced by the endogenous mitochondrial inhibitor malonate. *J Neurochem* **61**:1147-1150.

Beal MF, Henshaw DR, Jenkins BG, Rosen BR, and Schulz JB (1994) Coenzyme Q10 and nicotinamide block striatal lesions produced by the mitochondrial toxin malonate. *Ann Neurol* **36**:882-888.

Bernardi P (1999) Mitochondrial transport of cations: channels, exchangers, and permeability transition. *Physiol Rev* **79**:1127-1155.

Biswas SC, Ryu E, Park C, Malagelada C, and Greene LA (2005) . Puma and p53 play required roles in death evoked in a cellular model of Parkinson disease. *Neurochem Res* **30**:839-845.

Brouillet E, Hantraye P, Ferrante RJ, Dolan R, Leroy-Willig A, Kowall NW, and Beal MF (1995) Chronic mitochondrial energy impairment produces selective striatal degeneration and abnormal choreiform movements in primates. *Proc Natl Acad Sci USA* **92**:7105-7109.

Browne SE, and Beal MF (2002) Toxin-induced mitochondrial dysfunction. *Int Rev Neurobiol* **53**:243-279.

Cao G, Minami M, Pei W, Yan C, Chen D, O'Horo C, Graham SH, and Chen J (2001) Intracellular Bax translocation after transient cerebral ischemia: implications for a role of the mitochondrial apoptotic signaling pathway in ischemic neuronal death. *J Cereb Blood Flow Metab* **21**:321-333.

Cao J, Semenova MM, Solovyan VT, Han J, Coffey ET, and Courtney MJ (2004) Distinct requirements for p38alpha and c-Jun N-terminal kinase stress-activated protein kinases in different forms of apoptotic neuronal death. *J Biol Chem* **279**:35903-35913.

Choi WS, Eom DS, Han BS, Kim WK, Han BH, Choi EJ, Oh TH, Markelonis GJ, Cho JW, Oh YJ (2004) Phosphorylation of p38 MAPK induced by oxidative stress is linked to activation of both caspase-8- and -9-mediated apoptotic pathways in dopaminergic neurons *J Biol Chem* **279**:20451-20460.

De Chiara G, Marcocci ME, Torcia M, Lucibello M, Rosini P, Bonini P, Higashimoto Y, Damonte G, Armirotti A, Amodei S, Palamara AT, Russo T, Garaci E, and Cozzolino F (2006) Bcl-2 Phosphorylation by p38 MAPK: identification of target sites and biologic consequences *J Biol Chem* **279**:14016-14023.

Düßmann H, Rehm M, Kögel D, and Prehn JHM (2003) Mitochondrial membrane permeabilization and superoxide production during apoptosis. A single-cell analysis *J. Biol Chem* **278**:12645-12649.

Esterbauer H, Schaur RJ, and Zollner H (1991) Chemistry and biochemistry of 4-hydroxynonenal, malonaldehyde and related aldehydes *Free Radic Biol Med* **11**:81-128.

Ferger B, Eberhardt O, Teismann P, de Groote C, and Schulz JB (1999) Malonate-induced generation of reactive oxygen species in rat striatum depends on dopamine release but not on NMDA receptor activation. *J Neurochem* **73**:1329-1332.

Fernandez-Gomez FJ, Galindo MF, Gomez-Lazaro M, Yuste VJ, Comella JX, Aguirre N, and Jordan J (2005) Malonate induces cell death via mitochondrial potential collapse and delayed swelling through an ROS-dependent pathway. *Br J Pharmacol* **144**:528-537.

Fernandez-Gomez FJ, Pastor MD, Garcia-Martinez EM, Melero-Fernandez de Mera R, Gou-Fabregas M, Gomez-Lazaro M, Calvo S, Soler RM, Galindo MF, Jordan J. (2006) Pyruvate protects cerebellar granular cells from 6-hydroxydopamine-induced cytotoxicity by activating the Akt signaling pathway and increasing glutathione peroxidase expression. *Neurobiol Dis* **24**:296-307.

Ghatan S, Lerner S, Kinoshita Y, Hetman M, Patel L, Xia Z, Youle RJ, and Morrison RS (2000) p38 MAP kinase mediates bax translocation in nitric oxide-induced apoptosis in neurons. *J Cell Biol* **150**:335-347.

Goldstein JC, Waterhouse NJ, Juin P, Evan GI, and Green DR (2002) The coordinate release of cytochrome c during apoptosis is rapid, complete and kinetically invariant. *Nat Cell Biol* **2**:156-162.

Gomez-Lazaro M, Fernandez-Gomez FJ, and Jordan J (2004) p53: twenty five years understanding the mechanism of genome protection. *J Physiol Biochem* **60**:287-307.

Goping IS, Gross A, Lavoie JN, Nguyen M, Jemmerson R, Roth K, Korsmeyer SJ, and Shore GC (1998) Regulated targeting of BAX to mitochondria. *J Cell Biol* **143**:207-215.

Green DR (2006) At the gates of death. *Cancer Cell* **9**:328-330.

Jordan J, Cena V, and Prehn JH (2003) Mitochondrial control of neuron death and its role in neurodegenerative disorders. *J Physiol Biochem* **59**:129-141.

Jordan J, Galindo MF, Tornero D, Gonzalez-Garcia C, and Cena V (2004) Bcl-xL blocks mitochondrial multiple conductance channel activation and inhibits 6-OHDA-induced death in SH-SY5Y cells. *J Neurochem* **89**:124-133.

Karpinich NO, Tafani M, Rothman RJ, Russo MA, and Farber JL (2002) The course of etoposide-induced apoptosis from damage to DNA and p53 activation to mitochondrial release of cytochrome c. *J Biol Chem* **277**:16547-16552.

Khaled AR, Kim K, Hofmeister R, Muegge K, and Durum SK (1999) Withdrawal of IL-7 induces Bax translocation from cytosol to mitochondria through a rise in intracellular pH. *Proc Natl Acad Sci USA* **96**:14476-14481.

Kuwana T, Bouchier-Hayes L, Chipuk JE, Bonzon C, Sullivan BA, Green DR, and Newmeyer DD (2005) BH3 domains of BH3-only proteins differentially regulate Bax-mediated mitochondrial membrane permeabilization both directly and indirectly *Mol Cell* **17**:525-535.

Lin CH, Lu YZ, Cheng FC, Chu LF, and Hsueh CM (2005) Bax-regulated mitochondria-mediated apoptosis is responsible for the in vitro ischemia induced neuronal cell death of Sprague Dawley rat. *Neurosci Lett* **387**:22-27.

Lombard DB, Chua KF, Mostoslavsky R, Franco S, Gostissa M, and Alt FW (2005) DNA repair, genome stability, and aging. *Cell* **120**:497-512.

Luetjens CM, Bui NT, Sengpiel B, Münstermann G, Poppe M, Krohn AJ, Bauerbach E, Krieglstein J, and Prehn JHM (2000) Delayed mitochondrial dysfunction in excitotoxic neuron death: cytochrome c release and a secondary increase in superoxide production *J Neurosci* **20**:5715-5723.

Martinou JC, Desagher S, and Antonsson B (2002) Cytochrome c release from mitochondria: all or nothing. *Nat Cell Biol* **2**:E41-43.

Mattson MP and Kroemer G (2003) Mitochondria in cell death: novel targets for neuroprotection and cardioprotection. *Trends Mol Med* **9**:196-205.

Poppe M, Reimertz C, Munstermann G, Kogel D, and Prehn JH (2002) Ceramide-induced apoptosis of D283 medulloblastoma cells requires mitochondrial respiratory chain activity but occurs independently of caspases and is not sensitive to Bcl-xL overexpression *J Neurochem* **82**:482-494.

Putcha GV, Deshmukh M, and Johnson EMJr (1999) BAX translocation is a critical event in neuronal apoptosis: regulation by neuroprotectants, BCL-2, and caspases. *J Neurosci* **19**:7476-7485.

Sanchez-Prieto R, Sanchez-Arevalo VJ, Servitja JM, and Gutkind JS (2002) Regulation of p73 by c-Abl through the p38 MAP kinase pathway. *Oncogene* **21**:974-979.

Schulz JB, Weller M, Matthews RT, Heneka MT, Groscurth P, Martinou JC, Lommatzsch J, von Coelln R, Wullner U, Loschmann PA, Beal MF, Dichgans J, and Klockgether T (1998) Extended therapeutic window for caspase inhibition and synergy with MK-801 in the treatment of cerebral histotoxic hypoxia. *Cell Death Differ* **5**:847-857.

Sharpe JC, Arnoult D, and Youle RJ (2004) Control of mitochondrial permeability by Bcl-2 family members. *Biochim Biophys Acta* **1644**:107-113.

Uo T, Kinoshita Y, and Morrison RS (2005) Neurons exclusively express N-Bak, a BH3 domain-only Bak isoform that promotes neuronal apoptosis *J Biol Chem* **280**:9065-9073.

Waterhouse NJ, Goldstein JC, von Ahsen O, Schuler M, Newmeyer DD, and Green DR (2001) Cytochrome c maintains mitochondrial transmembrane potential and ATP generation after outer mitochondrial membrane permeabilization during the apoptotic process. *J Cell Biol* **153**:319-328.

Wolter KG, Hsu YT, Smith CL, Nechushtan A, Xi XG, and Youle RJ (1997) Movement of Bax from the cytosol to mitochondria during apoptosis. *J Cell Biol* **139**:1281-1292.

Wong S, McLaughlin J, Cheng D, and Witte ON (2003) Cell context-specific effects of the BCR-ABL oncogene monitored in hematopoietic progenitors *Blood* **101**:4088-4097.

FOOT NOTES

*This study was supported by SAF2002-04721 and SAF2005-07919-C02-01 from CICYT and 04005-00 Consejería de Sanidad from Junta de Comunidades de Castilla La Mancha to J.J. Ministerio de Sanidad y Consumo, Fundació La Caixa and Generalitat de Catalunya to J.X.C. and Science Foundation Ireland grant 03/RP1/B344 to JHMP. M. G-L and F.J. F-G are fellows from JCCM.

Person to receive reprint request

Joaquin Jordán, Grupo de Neurofarmacología. Departamento de Ciencias Médicas. Facultad de Medicina. Universidad Castilla-La Mancha. 02006-Albacete. Spain. Tel 34-967599200. Fax 34-967599327. E-Mail Joaquin.jordan@uclm.es

Legends for figures

Fig.1. Malonate induces apoptosis and activates mitochondrial apoptosis pathway in SH-SY5Y cells. A. Kinetics of malonate treatment on caspase-3 protein cleavage. Cells cultures were challenged with 50 mM malonate for the indicated times. Cells were then collected and total protein was extracted. Caspase-3 protein levels were determined by Western blot analysis. B. Cell cultures were co-transfected with GFP and Bcl-2, Bcl-X_L, p35 or Casp9 DN 24 h before malonate exposures. Cell viability was performed by studying the state of chromatin using Hoechst 33342 staining in GFP-positive cells 12 h after malonate addition. Each column represents the average obtained from four independent experiments.

Fig. 2. Malonate induces GFP-Bax translocation to mitochondria. A. SH-SY5Y cells were transfected with GFP-Bax using LipofectamineTM as described in Materials and Methods and were incubated for 24 h to allow for sufficient GFP-Bax expression and treated with 50 mM malonate. By 12 h after insults cells were fixed in 4 % paraformaldehyde. Confocal images were captured using a 63 X oil immersion lens. GFP-Bax demonstrated primarily diffuse staining in control (upper panel), while by 12 h after 50 mM malonate treatments a punctate pattern is evident (lower panel). Mito Track red staining was used to study the mitochondrial distribution. The images shown are representative of results obtained in four separate experiments, each performed in triplicate. Histograms represent the values of GFP-Bax fluorescence standard deviation (B) and GFP-Bax distribution patterns (C) in SH-SY5Y cells. D. Bax mediates mitochondrial transmembrane potential disruption. By 12 h after 50 mM treatment TMRE fluorescence intensities were analyzed to study $\Delta\Psi_m$ changes from cells with either a punctuate or diffuse GFP-Bax distribution challenged or not

with malonate. E. At 12 hours of 50 mM malonate treatment, GFP-Bax cells with a punctuate pattern after malonate present fragmented chromatin (arrows). Hoechst 33342 dye was added to study the state of chromatin. GFP-Bax was captured in the FITC channel (upper panel) and Hoechst 33342 was captured in the DAPI channel (lower panel). Results are presented as mean \pm S.D.; they are representative of at least three experiments, each performed in triplicate. $**p < 0.01$ and $***p < 0.001$ versus control conditions.

Fig.3. Bax is required for malonate- induce apoptosis. A-B. Three h before malonate (50mM) addition cells were treated with furosemide (10 μ M) and by 12 h after insult fixed in 4 % paraformaldehyde. A. Confocal images were captured and GFP-Bax fluorescence distribution patterns were analyzed. B. Percent of apoptotic nuclei from SH-SY5Y cells cultures were determined by analyzing morphological state of the chromatin stained with Hoechst. C. Kinetics of malonate treatment on caspase-3 protein cleavage. Cell cultures were challenged with 50 mM malonate for the indicated times. Cells from MEF wild type (WT) and Bax^{-/-} mice (KO) cultures were then collected and total protein was extracted. Caspase-3 protein levels were determined by Western blot analysis at the indicated times. D. Bax protein expression is required for malonate-induced cell death. MEF wt and Bax^{-/-} cells were treated with 50 mM malonate. By 12 h after addition the percent of apoptotic nuclei was determined analyzing the state of the chromatin using Hoechst 33348. Results are presented as mean \pm S.D.; they are representative of at least three experiments, each performed in triplicate. $***p < 0.001$ versus control conditions.

Fig. 4. Vitamin E inhibits ROS induction, GFP-BAX translocation and cell death in response to malonate. Cells were pre-treated with 50 μ M vitamin E for one h and then 50 mM malonate was added to the culture media. A. ROS production was determined by measuring DCF fluorescence in a Spectra Max Gemini XS microplate reader. For GFP-BAX translocation and cell death experiments, cells were fixed with 4 % paraformaldehyde and confocal images of GFP-Bax fluorescence distribution patterns were captured with an epifluorescence microscope. Punctuated GFP-bax distribution was determined and expressed as percent of GFP-Bax transfected cells (B). C-D. Percent of apoptotic nuclei from SH-SY5Y (C) or cerebellar granular (D) cells cultures were determined by analyzing morphological state of the chromatin stained with Hoechst. SH-SY5Y cell cultures were pre-treated for 12 h with 10 μ M SKF86002 before malonate addition. Results are presented as mean \pm S.D.; they are representative of at least three experiments, each performed in triplicate. * $p < 0.05$; **, $p < 0.01$, *** $p < 0.001$ versus control conditions.

Fig. 5. Malonate-induced apoptosis is p53 independent. A. Whole-cell extracts from SH-SY5Y cells treated with or without malonate (50 μ M) were subjected to Western blotting technique and probed with an anti-p53 antibody. Cell cultures challenged for 6h with 100 μ M 6-hydroxydopamine (6OD) were used as positive control. Similar results were achieved in three independent experiments. B. MEF wt and p53^{-/-} cells were treated with 50 mM malonate. By 12 h after addition the percent of apoptotic nuclei was determined by analyzing the state of the chromatin using Hoechst 33348. Results are presented as mean \pm S.D.; they are representative of at least three experiments, each performed in triplicate.

Fig. 6. Malonate-induced apoptosis is mediated via p38 MAPK. A. Immunoblot showing phospho-p38 MAPK levels in 50 mM malonate-challenged SH-SY5Y cell extracts. B. SH-SY5Y cells were transfected with GFP-Bax and were incubated for 24 h to allow for sufficient GFP-Bax expression and treated with 50 mM malonate. By 12 h before insults cells were treated with SKF86002 (10 μ M) and by 12 h after malonate addition fixed in 4 % paraformaldehyde. Confocal images were captured in a 63 \times oil immersion lens and GFP-Bax distribution patterns (B) and GFP-bax fluorescence standard deviation (C) were analyzed. D. Cell viability was performed by studying the state of chromatin using Hoechst 33342 staining 12 h after malonate addition. Results are presented as mean \pm S.D.; they are representative of at least three experiments, each performed in triplicate. ** $p < 0.01$; *** $p < 0.001$ versus control conditions.

Fig. 7. A. Immunoblot showing phospho-p38 MAPK levels from 50 mM malonate-challenged SH-SY5Y cell extracts pretreated with 50 μ M vitamin E (Vit E) for the indicated times. Controls were treated with vehicle. B. Levels of MDA in cell cultures were determined after 12 h after 50 mM malonate addition. SH-SY5Y cell cultures were pre-treated for 12 h with 10 μ M SKF86002 before malonate addition. Bax-deficient MEFs were included to study the effect of *bax* gene deletion on MDA formation. C. Effects of pre-treatment with vitamin E (1h, 50 μ M) and SKF86002 (12 h, 10 μ M) on ROS production in SH-SY5Y neuroblastoma cells 1 h (early increase) and 12 h (late increase) after malonate addition. Results are presented as mean \pm S.D.; they are representative of at least three experiments, each performed in triplicate. * $p < 0.05$; **, $p < 0.01$, *** $p < 0.001$.

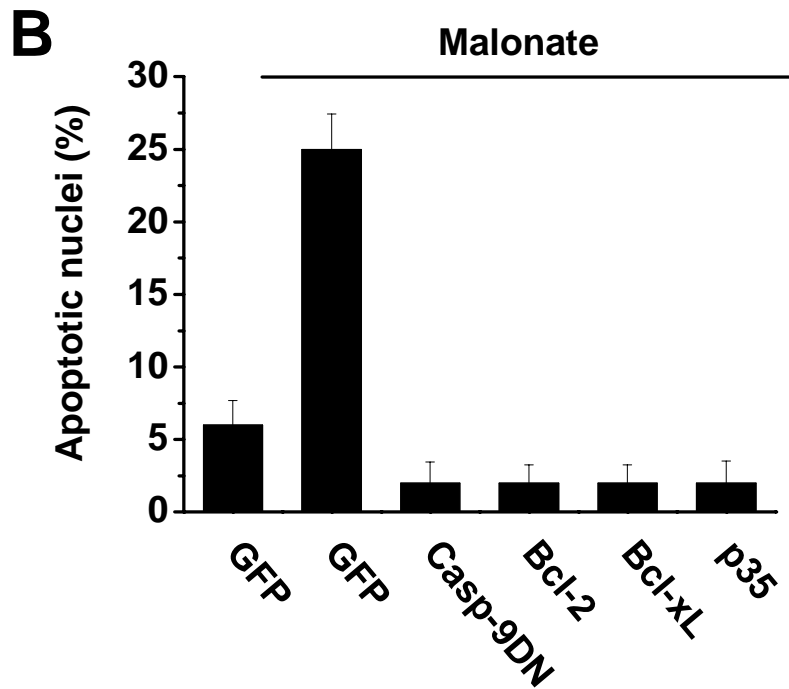
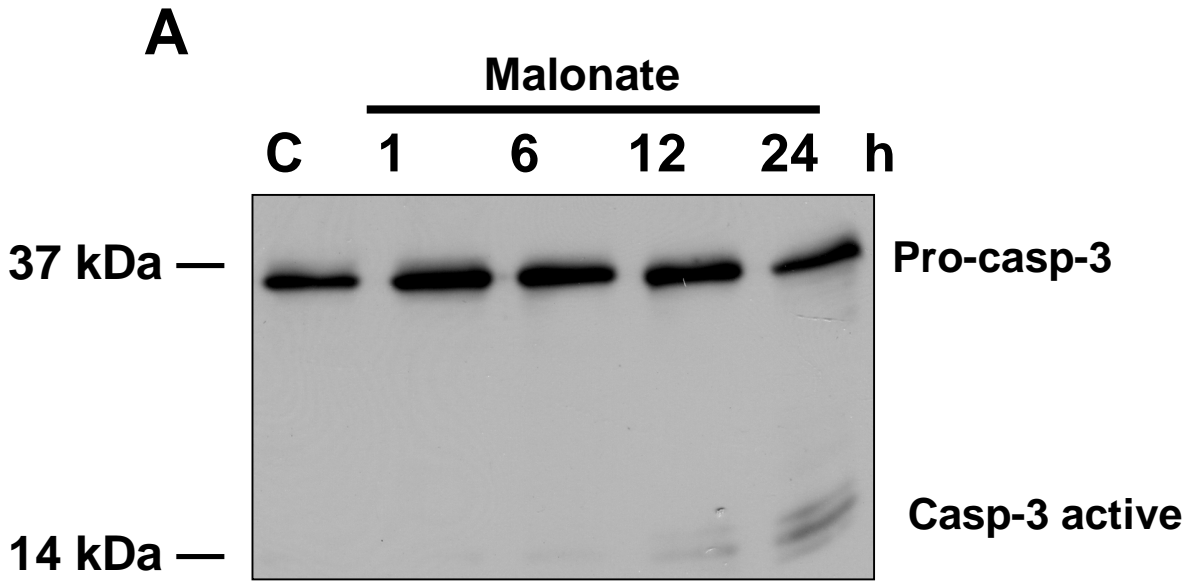
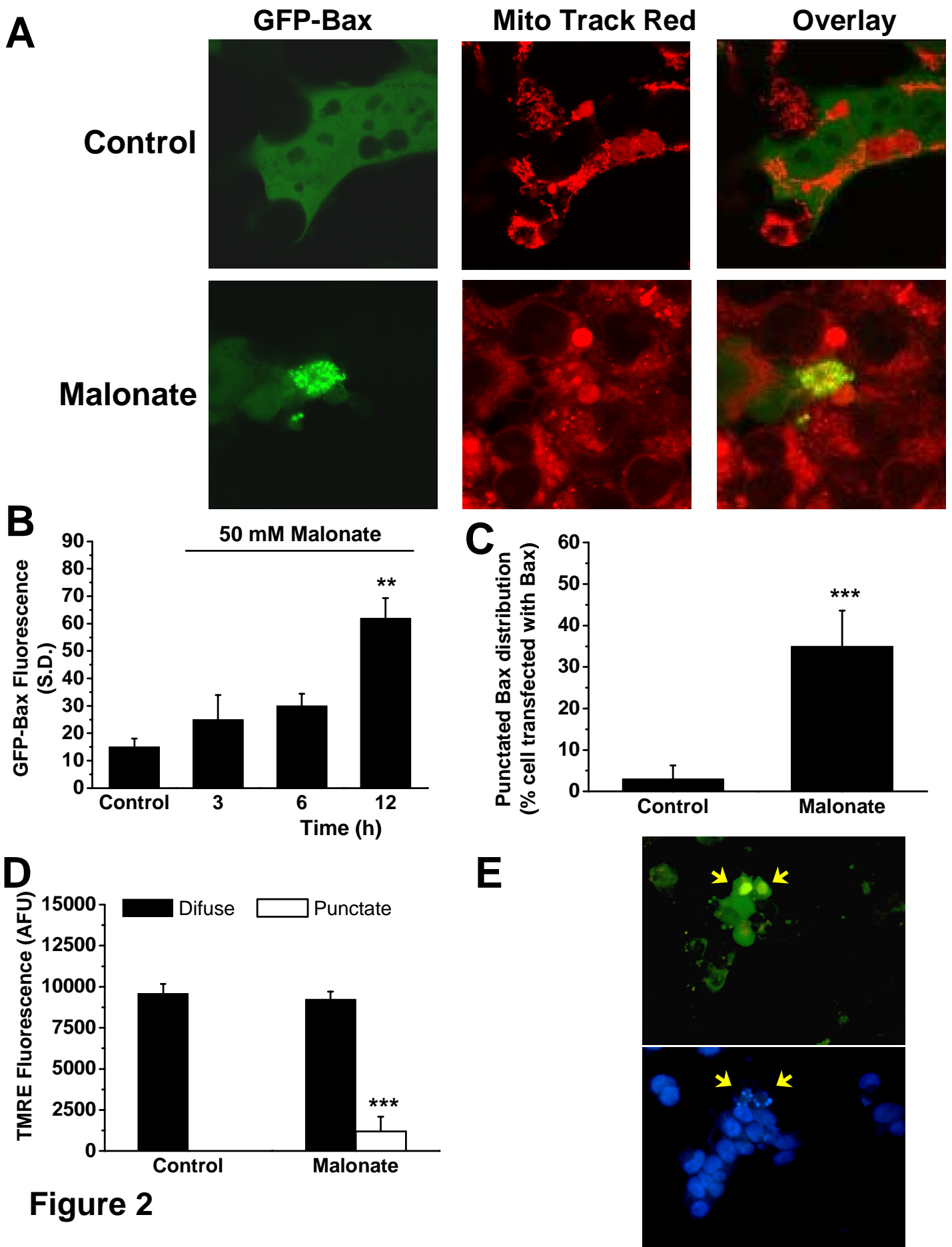


Figure 1



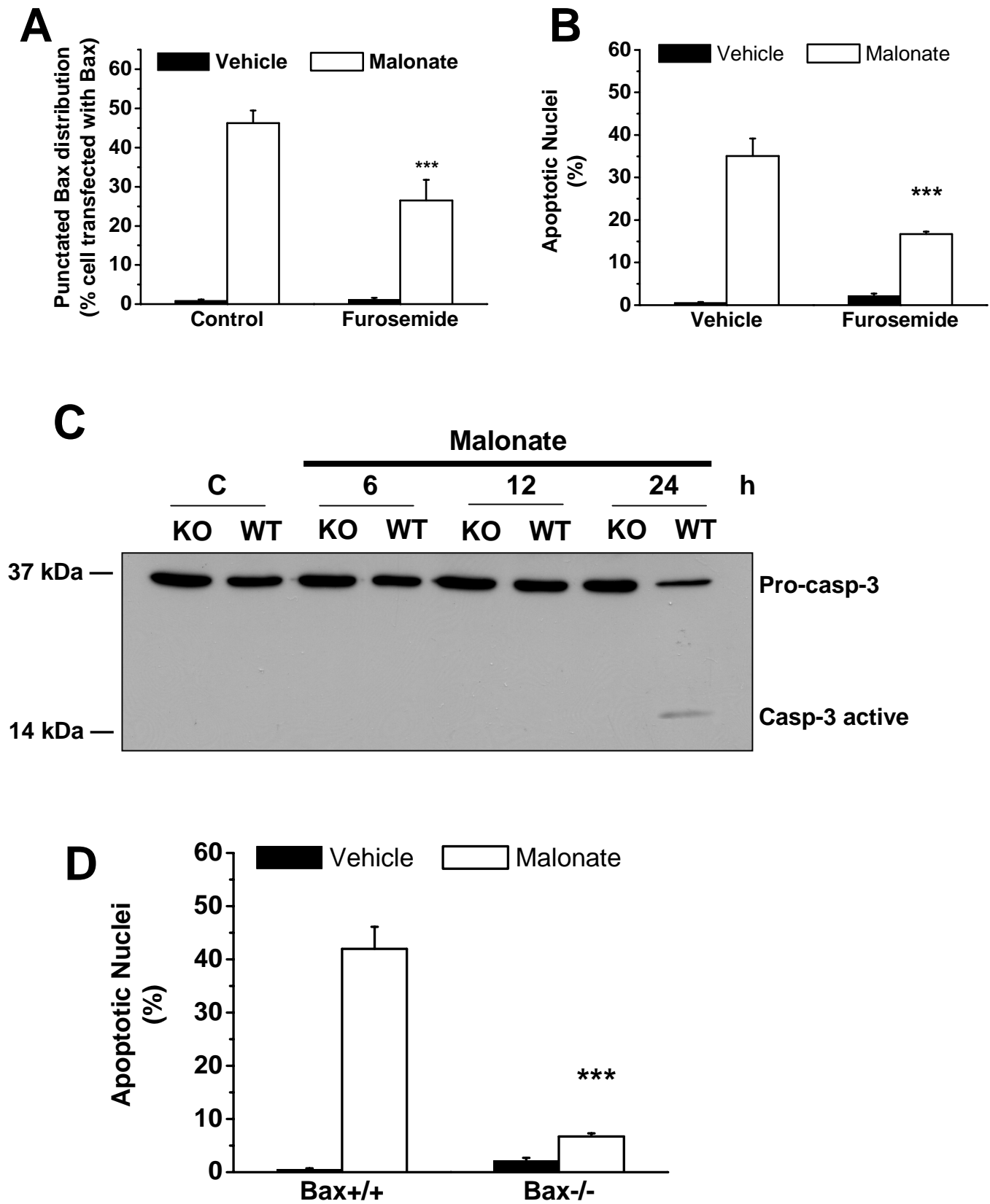


Figure 3

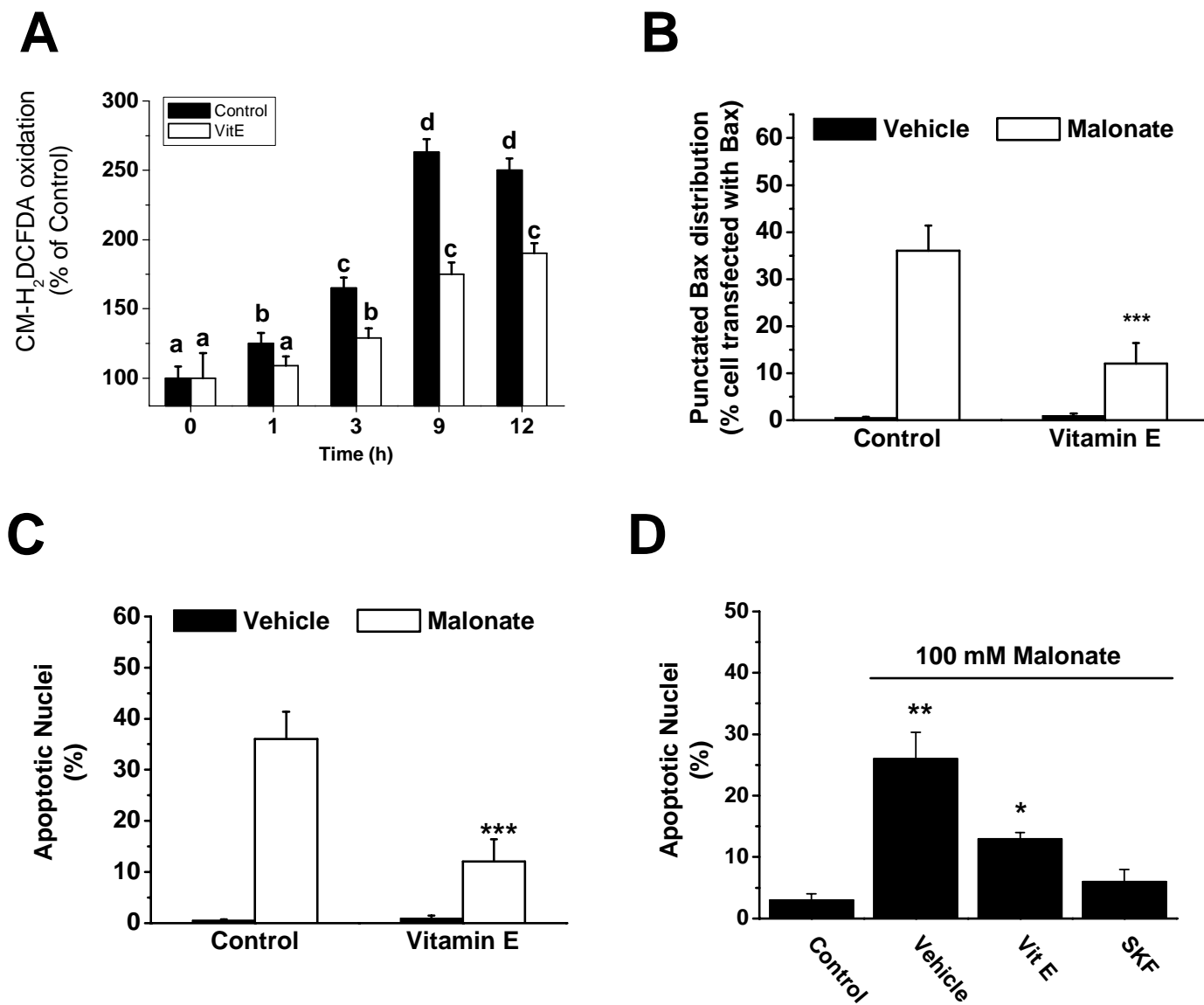


Figure 4

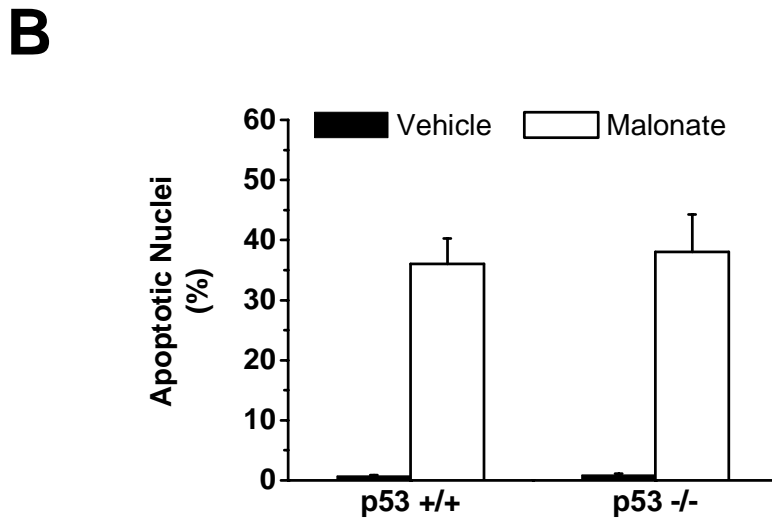


Figure 5

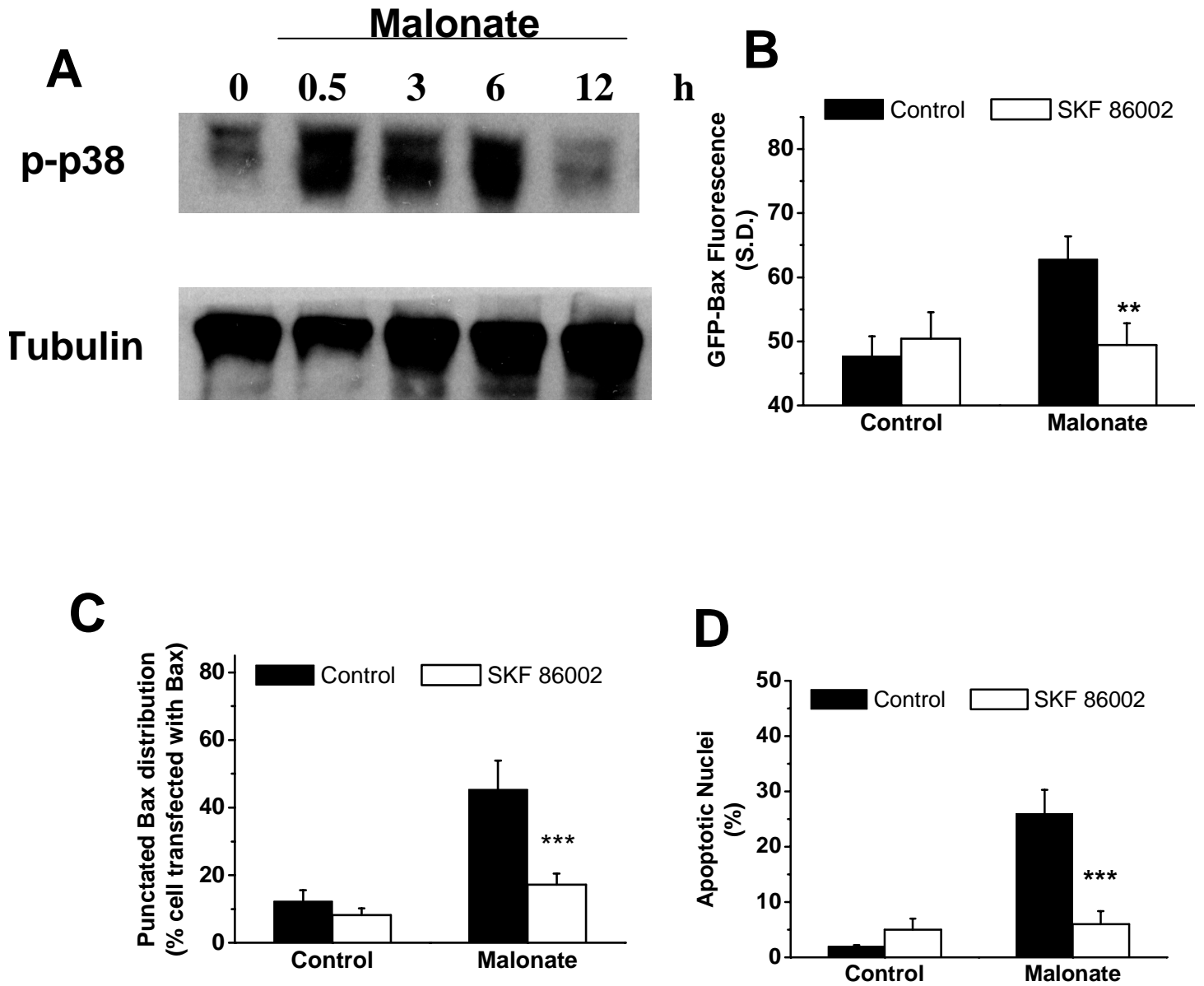


Figure 6

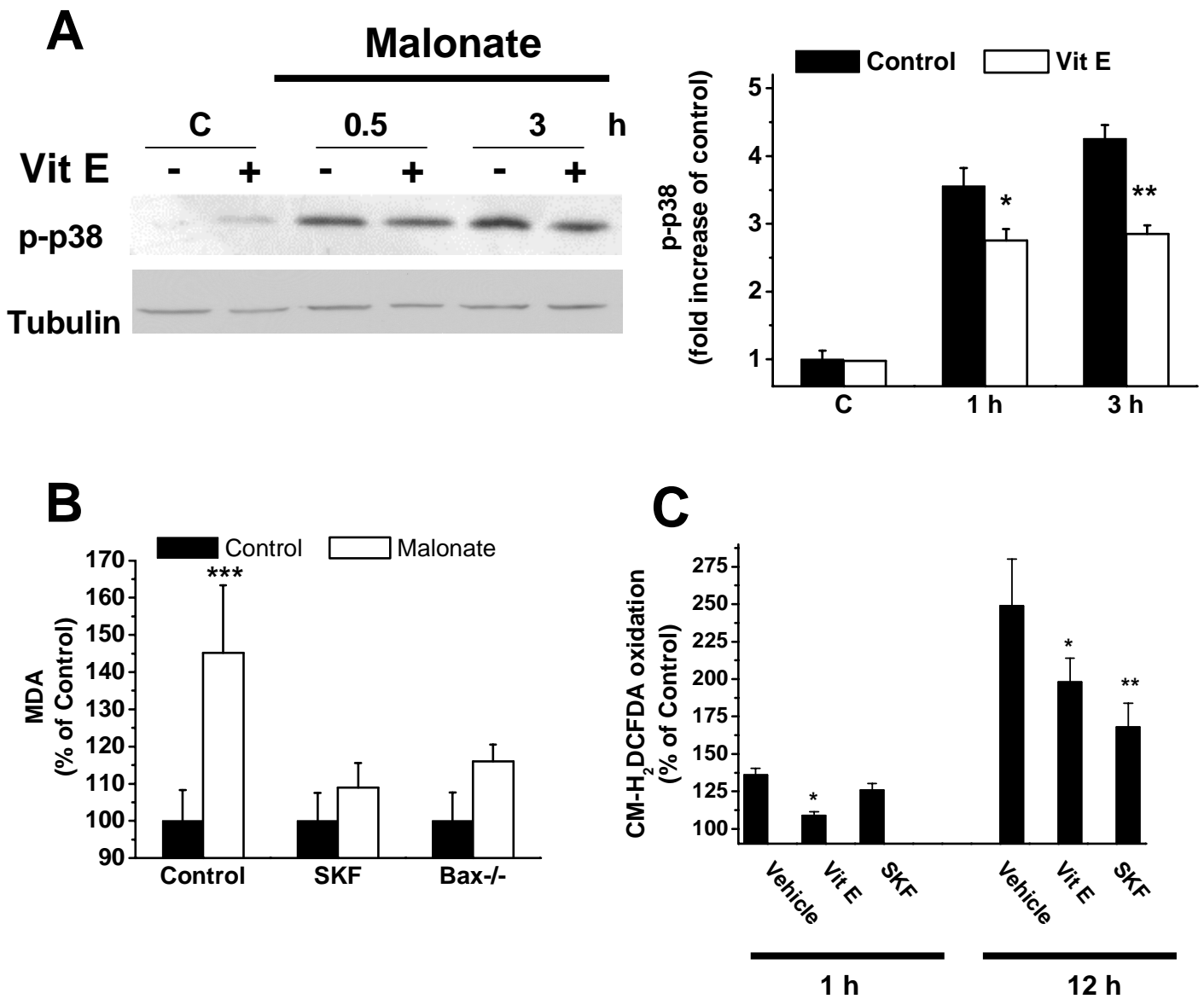


Figure 7